View metadata, citation and similar papers at core.ac.uk
brought to you by CORE
provided by Scholarship@Western

Western University
Scholarship@Western

Medical Biophysics Publications | Medical Biophysics Department

3-28-2015

Impact of Incremental Perfusion Loss on Oxygen Transport in a Capillary Network Mathematical Model.

Graham M Fraser

Michael D Sharpe

Daniel Goldman

Christopher G Ellis

Follow this and additional works at: https://ir.lib.uwo.ca/biophysicspub

Part of the Medical Biophysics Commons

Citation of this paper:

Fraser, Graham M; Sharpe, Michael D; Goldman, Daniel; and Ellis, Christopher G, "Impact of Incremental Perfusion Loss on Oxygen Transport in a Capillary Network Mathematical Model." (2015). *Medical Biophysics Publications*. 48.
https://ir.lib.uwo.ca/biophysicspub/48

Accepted Article

Received Date : 10-Jul-2014

Revised Date : 01-Mar-2015

Accepted Date : 24-Mar-2015

Article type : Original Research

Title: Impact of Incremental Perfusion Loss on Oxygen Transport in a Capillary Network Mathematical Model

Authors: Graham M. Fraser[1], PhD; Michael D. Sharpe[2], MD; Daniel Goldman[1], PhD; Christopher G. Ellis[1], PhD

1. Department of Medical Biophysics, University of Western Ontario

2. Department of Anesthesia and Perioperative Medicine, Critical Care Western, The University of Western Ontario, London Health Sciences Center, London, Ontario, Canada

Institution: University of Western Ontario

Sources of Funding: Canadian Institutes of Health Research MOP 102504 (Dr. Ellis) and the National Institute of Health HL089125 (Dr. Ellis and Dr. Goldman).

This article has been accepted for publication and undergone full peer review but has not been through the copyediting, typesetting, pagination and proofreading process, which may lead to differences between this version and the Version of Record. Please cite this article as doi: 10.1111/micc.12202

This article is protected by copyright. All rights reserved.

Accepted Article

Contact Address: Graham Fraser
University of Western Ontario
Medical Sciences Building 411
London Ontario
N6A 5C1

Contact Email Address: gmfraser@uwo.ca

Contact Phone Number: 519-661-2111 x85867

ABSTRACT

Objectives: To quantify how incremental capillary perfusion loss, such as that seen in experimental models of sepsis, affects tissue oxygenation using a computation model of oxygen transport.

Methods: A computational model was applied to capillary networks with dimensions 84x168x342 (NI) and 70x157x268 (NII) μm, reconstructed *in vivo* from rat skeletal muscle. Functional capillary density (FCD) loss was applied incrementally up to ~40% and combined with high tissue oxygen consumption to simulate severe sepsis.

Results: A loss of ~40% FCD loss decreased median tissue PO_2 to 22.9 and 20.1 mmHg in NI and NII compared to 28.1 and 27.5 mmHg under resting conditions. Increasing red blood cell supply rate (SR) to baseline levels returned tissue PO_2 to within 5% of baseline. High consumption combined with a 40% FCD loss, resulted in tissue anoxia in both network volumes and median tissue PO_2 of 11.5 and 8.9 mmHg in NI and NII respectively; median tissue PO_2 was recovered to baseline levels by increasing total SR 3 – 4 fold.

This article is protected by copyright. All rights reserved.

Conclusions: These results suggest a substantial increase in total SR is required in order to compensate for impaired oxygen delivery as a result of loss of capillary perfusion and increased oxygen consumption during sepsis.

KEYWORDS

sepsis; oxygen delivery; functional capillary density; blood flow; oxygen transport

ABBREVIATIONS USED

3D, three-dimensional; EDL, extensor digitorum longus; FCD, functional capillary density; NI, network I; NII, network II; PO_2, partial pressure of oxygen; RBC, red blood cell; SO_2, oxygen saturation; SR, supply rate;

INTRODUCTION

Mortality from sepsis and septic shock remains high despite improved diagnosis using biomarkers [21] and implementation of goal directed therapy [22,24,25]. Sepsis has been defined as a systemic inflammatory response to a bacterial infection [4] and is a common cause of mortality in a range of patient groups. Observable changes to blood flow within the microcirculation have been identified clinically within hours of infection onset [29]. Dysfunctional microvascular blood flow has been identified in animal models as a characteristic associated with the systemic inflammation in experimental sepsis; the most

This article is protected by copyright. All rights reserved.

Accepted Article

Accepted Article

notable aspect of blood flow disruption in these models is the loss of capillary perfusion in tissue remote to the site of infection [2,20]. The loss of perfused capillaries in the microvasculature impairs oxygen delivery and is followed by deleterious effects caused by hypoxia in living tissue [6]. Inadequate oxygen delivery in sepsis has therefore been hypothesized as a factor contributing to multiorgan dysfunction and patient mortality and as such has received considerable attention from researchers and clinicians.

Experimental models have shown varying degrees of perfusion loss in skeletal muscle, liver, brain and intestinal microcirculation [1,6,27,28]. The challenge of making direct measurements of tissue oxygen *in vivo* has led to the use of computer models in order to quantify how loss of capillary perfusion impacts oxygen delivery to living tissue. Previous modeling efforts by Goldman et al. utilized generated parallel capillary arrays and experimental measurements to provide a detailed description of oxygen tension within three-dimensional tissue volumes with loss of functional capillary density consistent with that observed in the skeletal muscle of a rat peritonitis model [12,13]. By adjusting tissue consumption in the model Goldman et al. matched observed oxygen extraction ratios from skeletal muscle capillaries. Goldman et al. concluded that increased consumption as predicted by the model and decreased oxygen supply would make tissue more susceptible to hypoxia in sepsis [13].

In a previous study we demonstrated that computer models using equivalent parallel capillary arrays result in higher estimates of tissue PO_2 when compared to capillary geometries reconstructed from intravital video recordings of blood flow *in vivo* [10]. The discrepancy between calculated tissue PO_2 in parallel arrays and reconstructed network geometries was shown under normal conditions as well as under simulated exercise,

This article is protected by copyright. All rights reserved.

Accepted Article

ischemia and hypoxia. We concluded that real network geometries reconstructed from experimental observations, produced oxygen transport solutions that more accurately represent the spatial PO_2 distribution and mean PO_2 values *in vivo* compared to equivalent parallel arrays generated using average measurements from the same experimental data sets. Given this result, computational models should utilize reconstructed or realistic network geometries, and corresponding experimental measurements of velocity, hematocrit and oxygen (SO_2 or PO_2) whenever possible.

In the present study we examine the impact of progressive functional capillary perfusion loss on oxygen transport in 3D reconstructed capillary networks. The impact of incremental FCD loss on oxygen delivery *in vivo* is not known, though computer models utilizing parallel arrays have shown decreased tissue PO_2 as a result of FCD loss [12,13]. By utilizing reconstructed networks we are able to simulate septic flow dysfunction in real capillary networks. Application of a physical flow model was used to determine blood flow redistribution resulting from stoppages in individual capillary segments. We then compared the resulting oxygen transport changes to solutions produced using baseline red blood cell supply rate produced from direct vessel-by-vessel hemodynamic and oxygen measurements made from the sample networks *in vivo*.

Recent clinical studies have monitored venous O_2 saturation in septic patients and used this metric as a target measurement for early goal directed therapies. Central venous SO_2 has been used as a trigger for blood transfusion and has been shown to improve through fluid resuscitation [22,24,26]. In the current study we were able to quantify how increasing red blood cell supply rate affects venular outflow saturation (SvO_2) from discrete

This article is protected by copyright. All rights reserved.

Accepted Article

capillary networks. The relationship between SvO_2 and restoration of basal tissue PO_2 levels can be related to clinical measurements of mixed venous saturation as a target for treatment of septic patients.

The objective of the present study is to quantify how varying degrees of FCD loss affect tissue oxygenation. Furthermore we aim to determine if increasing blood flow to hypoxic tissue will ameliorate oxygen delivery in the presence of increased oxygen consumption, a condition observed in experimental models of sepsis. Understanding how oxygen delivery is impaired in this model and how increased blood supply affects tissue oxygenation provides support to the concept of early goal directed therapy.

MATERIALS AND METHODS

3D Network Reconstruction

Two capillary networks from intravital microscopy of rat extensor digitorum longus muscle [20] that were reconstructed for a previous study [9], were used in blood flow and oxygen transport simulations; the methods of which have been described previously [9,30]. Briefly, video sequences of microvascular flow were processed to create functional images and overlapping fields of view and focal planes were registered to produce a mosaic map of the volume of interest. Characteristic features in each image were used for registration allowing for vessels to be tracked between images and focal planes. Vessels in each image were segmented using both manual and automated methods. Connections between vessel segments and at bifurcations were created using automated algorithms creating contiguous maps of network geometries. Completed geometries were processed with quality control software to ensure contiguous geometry, and appropriate proper flow directions as

This article is protected by copyright. All rights reserved.

Accepted Article

observed *in vivo*. Resulting vascular maps provide an accurate representation of the structure and transport conditions observed experimentally (as detailed below) in two discrete network volumes (see Table 1 for a summary of the network geometric data).

Capillary Hemodynamic and Oxygen Saturation Measurements

Individual vessels within each network geometry were analyzed to measure hematocrit, cell velocity and oxygen saturation using custom software package similar to that described previously [3,11,18]. Vessel segments were selected from functional images of microvascular flow [17] and space-time images [8] were created from 60 second long video sequences. Space-time images were used to measure cell velocity, hematocrit, and oxygen saturation using dual wavelength absorption spectroscopy [7,19]. Mean values measured for each vessel were indexed to the network geometry such that recorded data measured *in vivo* was paired with the specific capillary within the 3D geometry.

Modeling Flow in 3D Capillary Networks

Network reconstructions were processed to create a node-to-node description of the geometry for use in a steady state flow model [9]. Velocity and hematocrit values not measured experimentally were calculated using a mass balance to determine supply rate in parent and daughter vessels; this process was repeated in upstream segments as necessary to determine inflow node velocity, hematocrit, and supply rate. An existing steady state flow model [14] was applied using the flow equations described by Pries et al [23]. Inlet and outlet pressures were adjusted to approximate the specific velocity distribution

This article is protected by copyright. All rights reserved.

Accepted Article

observed in vivo and to create a starting point for further scaling of the flow model. RBC supply rates were recorded from the in vivo data in a cross section of the network and the total network RBC supply rate was determined. The pressure boundary conditions were incrementally adjusted until the RBC supply rate matched the experimentally measured values within < 0.1% [9].

In order to simulate the loss of functional capillary density (FCD) observed in the experimental models of sepsis, a subset of vessels were set to be stopped for a given perfusion loss using the following approach. Individual stop flow capillaries were randomly selected from the group of vessels within the network that intersected in projection with two sampling lines perpendicular to the network volume Y axis (Figure 1). Blood flow was arrested in the target vessels by increasing intra-capillary resistance such that the resulting flow solution calculated supply rate to be $< 10^{-4}$ of the original values in each of the target stop flow capillaries. Percent of FCD loss was calculated by counting the number of stopped flow vessels divided by the total number of vessels that intersected each sample line. Levels of FCD loss were created to approximately correspond to 10%, 20%, 30% and 40% FCD loss. The original pressure drop across the networks in the incremental perfusion loss simulations were held constant resulting in decreased supply rate with increasing FCD loss (Table 2 and 3). Longitudinal capillary point density for all levels of FCD loss, calculated as described previously[10], are shown in Figure 2. Flow solutions were created as described previously for each network at four levels of FCD loss; the ~40% range of FCD loss at 1X, 2X, 3.5X and 4X baseline RBC supply rates; and control simulations by iteratively adjusting inflow pressures until the target supply rate in inflow vessels was reached [9]. A single counter current inlet vessel in Network II was held constant at the originally measured RBC

This article is protected by copyright. All rights reserved.

Accepted Article

supply rate for all network II simulations. Control conditions with 0% FCD loss and supply rate matched to the incremental perfusion loss cases, and high consumption cases at 1X, 2X, 3.5X, and 4X supply rate were generated and separate simulations were run as a comparison for the cases with FCD loss.

Oxygen Transport Model

Oxygen tension in tissue was calculated using a finite difference model of oxygen transport developed by Goldman and Popel [14] and described previously [9]. Flow solutions generated for each case described above were used as the input for the transport models in order to describe tissue PO_2 within the sample volumes under each simulated condition. Finite elements were defined for the entire volume resulting in a monotonic 2 μm grid spacing. The diffusion between individual volume elements was calculated at each time step yielding PO_2 for each volume element, *P(x,y,z,t),* as follows: [9,14].

$$\frac{\partial P}{\partial t} = \left[1 + \frac{c_{Mb}}{\alpha}\frac{dS_{Mb}}{dP}\right]^{-1} \left\{ D\nabla^2 P - \frac{1}{\alpha} M\left(P\right) + \frac{1}{\alpha} D_{Mb} c_{Mb} \nabla \cdot \left(\frac{dS_{Mb}}{dP}\nabla P\right)\right\} \quad (1)$$

where D, α, and $M(P)$ are the diffusion coefficient, solubility and consumption rate of O_2 respectively of the tissue. Myoglobin concentration (c_{Mb}), diffusivity (D_{Mb}), and saturation (S_{Mb}) are also addressed through Equation 1 where S_{Mb} is determined by $S_{Mb}(P) = P / (P + P_{50,Mb})$ where $S_{Mb}(P)$ is the myoglobin saturation at a given partial pressure and $P_{50,Mb}$ is the partial pressure at which myoglobin is 50% saturated. Oxygen levels in the blood were determined within each vessel at each axial location (ξ) using a convective mass balance equation that describes blood oxygen saturation $S(\xi,t)$:

This article is protected by copyright. All rights reserved.

Accepted Article

$$\frac{\partial S}{\partial t} = -u\frac{\partial S}{\partial \xi} - \frac{1}{\pi R}\left[C + \alpha_b \frac{dP_b}{dS}\right]^{-1} \oint j \cdot d\theta \tag{2}$$

where u is the mean blood velocity, R is capillary radius, j is the oxygen flux out of the capillary at the axial location (ξ,θ), C is the O_2-binding capacity of blood, P_b is the intracapillary PO_2 and α_b is the solubility of O_2 in plasma.

The flux of O_2 between capillaries and tissue is was defined as:

$$j = \kappa\left(P_b - P_w\right) \tag{3}$$

where κ is the mass transfer coefficient and P_w is the tissue PO_2 at the capillary surface. κ is a function of the capillary hematocrit in a given vessel and reflects the effect of red blood cell spacing on diffusional exchange between capillary and tissue [5]. The boundary condition at the capillary-tissue interface was specified as:

$$-D\alpha\frac{\partial P_w}{\partial n} = j \tag{4}$$

where n is the unit vector normal to the capillary surface and j is defined by Eq. 3. Boundary conditions at the tissue edges were specified as a zero flux boundary condition.

The above O_2 transport equations 1 – 4 were combined with Michaelis-Menten consumption kinetics, $M = M_0\, P/(P + P_{cr})$ and the Hill equation for oxyhemoglobin saturation, $S(P) = P^n/(P^n + P_{50}^n)$ to define O_2 transport within the 3D volume [15]. The baseline oxygen consumption rate, M_0, (Table 2 & 3) was selected such that the resulting capillary SO_2 throughout the network fit approximately with experimental observations. Simulations were ran from a starting state of zero PO_2 throughout the volume and diffusion was calculated between capillaries and tissue elements incorporating consumption for each

This article is protected by copyright. All rights reserved.

case as described in Table 2 and 3. Values for constants used in the equations above are listed in Table 4. Each simulation was run to a steady state condition established when the slope of tissue PO_2 over time in corner elements was equal to zero.

RESULTS

Steady state oxygen transport simulations were completed, for each reconstructed network geometry, under four incremental levels of functional capillary density loss with normal oxygen consumption conditions. Tissue PO_2 distributions calculated for each case under normal consumption are shown in Figure 3. Increasing FCD loss and a concomitant decrease in RBC supply rate resulted in a progressive reduction in median tissue PO_2 levels from baseline values of 28.1 mmHg and 27.5 mmHg for networks I and II respectively. At the highest level of FCD loss (40% for network I and 42.9% for network II) median tissue PO_2 was reduced to 22.9 mmHg, in network I, and 20.1 mmHg in network II. In both network geometries the highest level of FCD loss caused the span of the fourth quartile of PO_2 values to widen and tissue PO_2 values residing in the third quartile to fall below the median value at baseline (Figure 3). When boundary pressures were increased to restore RBC supply rate to baseline levels for 40.0% and 42.9% FCD loss, median tissue PO_2 increased to 26.7 mmHg in network I and 26.8 mmHg in network II; returning median PO_2 to within 5% of baseline levels.

Color PO_2 surface maps in Figure 5 illustrate PO_2 conditions with normal consumption in the network I sample volume under baseline and the resulting drop in PO_2 following a 40% FCD loss denoted in vessel maps by gray shaded segments. A substantial shift in the lower quartile was seen for both sample network volumes dropping from 23.8 and 25.0 mmHg

This article is protected by copyright. All rights reserved.

Accepted Article

under baseline conditions with normal consumption to 17.2 and 17.4 mmHg with a 40% FCD loss. The decrease in the lower quartile tissue PO_2 values for network I are clearly visualized in Figure 5 showing the fall of tissue PO_2 levels at the venous end of the network following the imposed perfusion loss and associated flow redistribution. Minimum tissue PO_2 fell to 13.5 and 15.4 mmHg compared to the baseline levels of 19.5 and 22.4 mmHg in networks I and II respectively. The lower left panel of Figure 5 shows the tissue PO_2 of network I with 40% FCD loss following RBC supply rates being restored to baseline. The lower quartile values for networks I and II with 40.0% and 42.9% FCD loss and restoration of baseline RBC supply rate increased tissue PO_2 to 22.04 and 24.5 mmHg, while minimum tissue PO_2 similarly increased to 18.9 and 22.5 mmHg respectively.

Mixed capillary outflow saturation (SvO_2) decreased progressively with increasing FCD loss. By imposing a 40.0% and 42.9% FCD loss the corresponding drop in RBC supply rate caused $SvO_2$to drop to 12.9 and 13.2 percent saturated compared to 23.8 and 26.9 percent saturated under baseline conditions. With baseline RBC supply rate restored in network I at 40.0% FCD loss and network II at 42.9% FCD loss, SvO_2 increased to 23.5 and 27.4 percent saturation in the two networks respectively.

A second set of steady state oxygen transport simulations were completed, for each network volume, with the highest level of FCD loss (40.0% and 42.9%) and double the baseline oxygen consumption, at incrementally increasing RBC supply rates (Figure 4). Median tissue PO_2 levels for double oxygen consumption and baseline RBC supply rate was 11.5 mmHg for network I and 8.9 mmHg for network II. The lower quartile for baseline RBC supply rate lay at 2.7 and 3.3 mmHg with simulations resulting in minimum PO_2 of 0.0 and

This article is protected by copyright. All rights reserved.

Accepted Article

Accepted Article

0.4 mmHg for network I and II respectively. A doubling of the baseline RBC supply rate was not sufficient to restore median tissue PO_2 levels in either network with the median rising to 20.6 and 22.6, lower quartiles of 11.7 and 19.7, and minimum tissue PO_2 of 9.8 and 15.0 mmHg in networks I and II respectively. A 3.5 fold increase in RBC supply rate restored median tissue PO_2 in network II (27.9 mmHg) whereas a 4-fold increase was necessary to restore baseline levels in network I (28.0 mmHg). Increasing RBC supply rate resulted in distinctly narrowed PO_2 distributions in each network volume, particularly in the second and third quartiles.

With doubled oxygen consumption rate and baseline RBC supply rate the SvO_2 fell to 0.0 and 0.4 percent saturation in networks I and II. Doubling RBC supply rate dramatically increased SvO_2 in both networks, restoring outflow saturations to 16.9 and 23.5 percent saturation in networks I and II respectively. Higher RBC supply rates resulted in SvO_2 well above baseline levels. The 3.5 fold increase in RBC supply rate caused SvO_2 of 34.5 percent saturation in network I and 38.6 percent saturation in network II, while 4 times baseline supply rate raised outflow saturations to 44.4 and 41.3 percent saturation in the two networks respectively.

Pressures needed to create RBC flux conditions in each simulation are shown in Table 2 and 3 for networks I and II respectively. Under baseline boundary pressures increasing perfusion loss (PL) resulted in decreased RBC supply rate in each network though supply rate decreases were dependent on individual vessels that were caused to stop and therefore did not create linear decreases in supply rate with increasing FCD loss. In order to increase RBC supply rate in the high consumption (HC) simulations it was necessary to increase

This article is protected by copyright. All rights reserved.

Accepted Article

boundary pressures such that the mean pressure drop increased by a factor larger than the scale of desired RBC supply rate increase.

DISCUSSION

Using real microvascular geometry, and associated experimental intravital microscopic measurements from rat extensor digitorum longus, we have shown how FCD loss with a concomitant decrease in RBC supply rate would impact tissue oxygenation. Further we have demonstrated that restoration of baseline RBC supply rate will restore original tissue PO_2 levels and that in order to compensate for increased metabolic consumption with FCD loss, it is necessary for blood flow to increase several fold. With normal consumption, the highest tested FCD loss caused up to a 27% decrease in median tissue PO_2 and a 31% decrease in minimum PO_2. By increasing the total RBC supply rate to the simulated tissue volume under normal consumption conditions and the highest level of FCD loss, median tissue PO_2 was restored to within < 5% below baseline, and minimum tissue PO_2 was returned to within 3% of baseline in network I. In network II, restoration of baseline RBC SR caused median tissue PO_2 to be increased to within 1% of baseline. Control simulations with no stopped vessels and RBC supply rates matched to the incremental FCD loss simulations showed decrease in tissue PO_2 comparable to the corresponding level of FCD loss; this suggests that in the absence of high consumption the decreased PO_2 was primarily due to impaired supply resulting from stopped flow vessels and not from higher diffusion distance to flowing capillaries. Furthermore, the presence of anastamoses between adjacent capillaries allow for blood flow to redistribute around stopped flow vessels limiting the impact a heterogeneous stoppage of capillaries may have on oxygen delivery.

This article is protected by copyright. All rights reserved.

Increased oxygen consumption in the presence of high FCD loss with baseline flow conditions caused a radical drop in tissue PO_2 creating anoxic regions in sample networks (Figure 4 & 6) and resulting in substantial hypoxia throughout the tissue volumes while reducing median tissue PO_2 to 41% (network I) and 32% (network II) of baseline levels. Under these conditions 26% of tissue elements in network I and 14% in network II had PO_2 levels below 3 mmHg. Cellular metabolism has been previously shown to decreases under hypoxic conditions in an oxygen dependent fashion when PO_2 drops below 2 mmHg [31]. However recent work by Wilson in isolated mitochondria [32] and Golub in skeletal muscle [16] found critical PO_2 (the partial pressure resulting in half maximal respiration) to be between 10 – 12 mmHg. By doubling RBC supply rate, tissue PO_2 was partially recovered in simulations for both network volumes, restoring tissue oxygen levels to 73% and 82% of baseline in networks I and II respectively and no tissue elements with PO_2 below 10 mmHg. In order to return median tissue PO_2 back to baseline under high consumption and high FCD loss conditions it was necessary to increase RBC supply rate by 4 fold in network I resulting in a tissue PO_2 99.6% of baseline while an increase of 3.5 fold was necessary in network II to restore median tissue PO_2 to 101% of baseline levels. This clearly illustrates that a substantial increase in RBC flux is necessary to compensate for the combination of observed FCD loss and the estimated high consumption present in microvascular septic injury. Control simulations that matched increases in RBC supply rates in the absence of FCD loss showed that a substantial proportion of the depressed tissue PO_2 was a result of increased diffusion distance in the ~40% FCD loss simulations indicating that perfusion loss combined with high consumption results in both a supply and diffusion limitation. The pressure increases required to raise supply rate supply rate in the high consumption simulations was 25 – 34% higher in the ~40% FCD loss cases than in controls (Table 2 and

Accepted Article

This article is protected by copyright. All rights reserved.

Accepted Article

3). This illustrates that meeting supply rate demands in the face of a large number of stopped flow vessels would require unusually high driving pressure.

In addition to tissue PO_2 we examined mixed capillary outflow saturations in each of the presented simulation cases. We found that progressive functional capillary density loss caused mixed capillary outflow saturation to decrease up to 50% compared to baseline. Decreases in mixed capillary outflow saturation can be compared with clinical findings that show a drop in mixed venous saturation in patients with severe sepsis which has also proven to be an indicator of higher patient mortality [25]. In the simulation cases where high consumption was used to simulate severe sepsis we found that increasing RBC supply rate by a factor of 2 restored median tissue PO_2 to within 18% - 27% below baseline and this was reflected in a similar recovery of SvO_2 to 14% - 29% below baseline values. However it is important to note that the blood flow increases needed to restore median tissue PO_2 to baseline levels increased SvO_2 to 40% - 87% higher than baseline levels.

Previously. Goldman et al. [12] utilized parallel capillary arrays to examine the effect of perfusion loss in sepsis and found that tissue PO_2 decreased in simulated average sepsis (tissue consumption $M_o = 3.86E\text{-}4$ mL O_2/mL/s) to a mean value of 35.4 mmHg from 43.0 mmHg in control cases. Our findings show a PO_2 of 10.3 – 11.5 mmHg in high consumption/high perfusion loss simulations versus 28.1 – 28.2 mmHg at baseline. There are two main reasons for the differences in mean tissue PO_2 determined in this study compared to previous findings. First, Goldman et al. utilized an inlet blood saturation of 69%, which is slightly higher than our experimentally measured value of 63% for the specific networks used in our simulations. Higher inlet saturation would result in slightly elevated tissue PO_2 than what our simulations predict. Second, the relative capillary density

This article is protected by copyright. All rights reserved.

Accepted Article

determined for the real networks used in the current study were 665 cap/mm^2 and 855 cap/mm^2 compared to the density chosen by Goldman et al. of 1000 cap/mm^2 and 1500 cap/mm^2. The high vascular density, blood velocities and hematocrit used to determine blood flow in the previous study result in much higher RBC supply rates than those used as the input for our simulations. Examination of our results in conjunction of Goldman's parallel arrays allows for a greater context of the delivery of oxygen *in vivo* in regions of varying vascularization and metabolic demand.

The modeling approach that we have outlined in the current work is a strong foundation for future efforts in studying the impact sepsis has on oxygen delivery as a result of microvascular injury and flow dysfunction. This approach provides a clearer picture of how perfusion loss and changes to metabolism affect tissue oxygenation, and the extent to which hypoxia may be present in tissue during a septic insult. Future improvements to the model will require precise maps of vascular geometry combined with direct measurements of individual vessels within the same geometry from septic animals *in vivo*. Previously outlined strategies for applying blood flow models to sparse hemodynamic data sets[9] combined with tracking the specific perfusion loss within a given geometry will provide a further context the current study is unable to provide. The current work represents the most realistic simulations that can be achieved without tracking loss of perfusion on a vessel-by-vessel basis, which would be the next step to fully characterize the impact of perfusion loss in vivo.

This article is protected by copyright. All rights reserved.

Accepted Article

CONCLUSION

We have described a comprehensive and detailed model of oxygen transport that utilizes capillary networks reconstructed from intravital videos of rat skeletal muscle combined with a flow model that allows hemodynamic and oxygen saturation measurements to accurately represent conditions measured in the network *in vivo*. This model of oxygen transport simulates the blood flow dysfunction observed in skeletal muscle during experimental sepsis and reproduces varying degrees of functional capillary density loss, increases in tissue oxygen consumption, and recovery of the tissue by increasing red blood cell supply rate. Further, we have related how capillary outflow saturation changes as a result of loss of perfusion and increased consumption. Our findings provide insight into how tissue oxygenation may be affected by flow dysfunction in sepsis and that tissue hypoxemic conditions caused by a loss of vessel perfusion can be recovered by increasing total tissue perfusion to simulation volumes.

PERSPECTIVE

The functional impact of capillary perfusion loss in human disease is still difficult to characterize. Examination of this problem in models of skeletal muscle provides a meaningful analog to conditions in vital organs that is important in and of itself given the physiological importance of skeletal muscle and the relative tissue mass that is potentially affected. While predictions for mixed capillary outflow saturation do not translate directly to central venous measurements made in patients, it does provide a tangible reference point that puts into context how changing vascular density, PO_2, and consumption in small vascular volumes might impact global measurements. While this work does elucidate how

This article is protected by copyright. All rights reserved.

Accepted Article

loss of perfused capillaries would impact tissue PO_2, the next step is to repeat our approach using data collected directly from septic animals, tracking the specific vessel loss, and directly calculating changes in consumption within observed discrete volumes. Collection of such a detailed data set, particularly from diseased animals, will remain a challenge. This will be a critical step in order to move this work forward and serves as strong motivation to carry out 3D reconstructions and modeling directly from an animal model of sepsis.

ACKNOWLEDGEMENTS

This project was supported by grants from the Canadian Institutes of Health Research MOP 102504 (C.G. Ellis) and the National Institute of Health HL089125 (D. Goldman and C.G. Ellis). The authors would also like to thank Stephanie Milkovich for her valuable contributions analyzing experimental data and reconstructing three-dimensional networks.

References

1. Albuszies G, Radermacher P, Vogt J, Wachter U, Weber S, Schoaff M, Georgieff M, Barth E. Effect of increased cardiac output on hepatic and intestinal microcirculatory blood flow, oxygenation, and metabolism in hyperdynamic murine septic shock. *Crit Care Med* **33**: 2332-2338, 2005.

2. Bateman RM, Sharpe MD, Ellis CG. Bench-to-bedside review: microvascular dysfunction in sepsis--hemodynamics, oxygen transport, and nitric oxide. *Critical care (London, England)* **7**: 359-373, 2003.

This article is protected by copyright. All rights reserved.

Accepted Article

3. Bateman RM, Sharpe MD, Goldman D, Lidington D, Ellis CG. Inhibiting nitric oxide overproduction during hypotensive sepsis increases local oxygen consumption in rat skeletal muscle. *Crit Care Med* **36**: 225-231, 2008.

4. Bone RC, Balk RA, Cerra FB, Dellinger RP, Fein AM, Knaus WA, Schein RM, Sibbald WJ. Definitions for sepsis and organ failure and guidelines for the use of innovative therapies in sepsis. The ACCP/SCCM Consensus Conference Committee. American College of Chest Physicians/Society of Critical Care Medicine. *Chest* **101**: 1644-1655, 1992.

5. Eggleton CD, Vadapalli A, Roy TK, Popel AS. Calculations of intracapillary oxygen tension distributions in muscle. *Mathematical biosciences* **167**: 123-143, 2000.

6. Ellis CG, Bateman RM, Sharpe MD, Sibbald WJ, Gill R. Effect of a maldistribution of microvascular blood flow on capillary O(2) extraction in sepsis. *Am J Physiol Heart Circ Physiol* **282**: H156-164, 2002.

7. Ellis CG, Ellsworth ML, Pittman RN. Determination of red blood cell oxygenation in vivo by dual video densitometric image analysis. *The American journal of physiology* **258**: H1216-1223, 1990.

8. Ellis CG, Ellsworth ML, Pittman RN, Burgess WL. Application of image analysis for evaluation of red blood cell dynamics in capillaries. *Microvascular research* **44**: 214-225, 1992.

9. Fraser GM, Goldman D, Ellis CG. Microvascular flow modeling using in vivo hemodynamic measurements in reconstructed 3D capillary networks. *Microcirculation* **19**: 510-520, 2012.

10. Fraser GM, Goldman D, Ellis CG. Comparison of generated parallel capillary arrays to three-dimensional reconstructed capillary networks in modeling oxygen transport in discrete microvascular volumes. *Microcirculation* **20**: 748-763, 2013.

This article is protected by copyright. All rights reserved.

Accepted Article

11. Fraser GM, Milkovich S, Goldman D, Ellis CG. Mapping 3-D functional capillary geometry in rat skeletal muscle in vivo. *Am J Physiol Heart Circ Physiol* **302**: H654-664, 2012.

12. Goldman D, Bateman RM, Ellis CG. Effect of sepsis on skeletal muscle oxygen consumption and tissue oxygenation: interpreting capillary oxygen transport data using a mathematical model. *Am J Physiol Heart Circ Physiol* **287**: H2535-2544, 2004.

13. Goldman D, Bateman RM, Ellis CG. Effect of decreased O2 supply on skeletal muscle oxygenation and O2 consumption during sepsis: role of heterogeneous capillary spacing and blood flow. *Am J Physiol Heart Circ Physiol* **290**: H2277-2285, 2006.

14. Goldman D, Popel AS. Computational modeling of oxygen transport from complex capillary networks. Relation to the microcirculation physiome. *Adv Exp Med Biol* **471**: 555-563, 1999.

15. Goldman D, Popel AS. A computational study of the effect of capillary network anastomoses and tortuosity on oxygen transport. *Journal of Theoretical Biology* **206**: 181-194, 2000.

16. Golub AS, Pittman RN. Oxygen dependence of respiration in rat spinotrapezius muscle in situ. *American journal of physiology Heart and circulatory physiology* **303**: H47-H56, 2012.

17. Japee SA, Ellis CG, Pittman RN. Flow visualization tools for image analysis of capillary networks. *Microcirculation* **11**: 39-54, 2004.

18. Japee SA, Pittman RN, Ellis CG. A new video image analysis system to study red blood cell dynamics and oxygenation in capillary networks. *Microcirculation* **12**: 489-506, 2005.

19. Japee SA, Pittman RN, Ellis CG. A new video image analysis system to study red blood cell dynamics and oxygenation in capillary networks. *Microcirculation* **12**: 489-506, 2005.

This article is protected by copyright. All rights reserved.

Accepted Article

20. Lam C, Tyml K, Martin C, Sibbald W. Microvascular perfusion is impaired in a rat model of normotensive sepsis. *J Clin Invest* **94**: 2077-2083, 1994.

21. Nguyen HB, Loomba M, Yang JJ, Jacobsen G, Shah K, Otero RM, Suarez A, Parekh H, Jaehne A, Rivers EP. Early lactate clearance is associated with biomarkers of inflammation, coagulation, apoptosis, organ dysfunction and mortality in severe sepsis and septic shock. *J Inflamm (Lond)* **7**: 6, 2010.

22. Ospina-Tascon G, Neves AP, Occhipinti G, Donadello K, Büchele G, Simion D, Chierego M-L, Silva TO, Fonseca A, Vincent J-L, De Backer D. Effects of fluids on microvascular perfusion in patients with severe sepsis. *Intensive Care Med* **36**: 949-955, 2010.

23. Pries AR, Secomb TW, Gessner T, Sperandio MB, Gross JF, Gaehtgens P. Resistance to blood flow in microvessels in vivo. *Circulation Research* **75**: 904-915, 1994.

24. Rivers E, Nguyen B, Havstad S, Ressler J, Muzzin A, Knoblich B, Peterson E, Tomlanovich M. Early goal-directed therapy in the treatment of severe sepsis and septic shock. *N Engl J Med* **345**: 1368-1377, 2001.

25. Rivers EP. Early goal-directed therapy in severe sepsis and septic shock: converting science to reality. *Chest* **129**: 217-218, 2006.

26. Rivers EP. Point: adherence to early goal-directed therapy: does it really matter? Yes. After a decade, the scientific proof speaks for itself. *Chest* **138**: 476-480; discussion 484-475, 2010.

27. Singer G, Stokes KY, Granger DN. Hepatic microcirculation in murine sepsis: role of lymphocytes. *Pediatr Surg Int* **24**: 13-20, 2008.

This article is protected by copyright. All rights reserved.

Accepted Article

28. Taccone FS, Su F, Pierrakos C, He X, James S, Dewitte O, Vincent J-L, De Backer D. Cerebral microcirculation is impaired during sepsis: an experimental study. *Critical care (London, England)* **14**: R140, 2010.

29. Trzeciak S, Dellinger RP, Parrillo JE, Guglielmi M, Bajaj J, Abate NL, Arnold RC, Colilla S, Zanotti S, Hollenberg SM, Investigators MAiRaS. Early microcirculatory perfusion derangements in patients with severe sepsis and septic shock: relationship to hemodynamics, oxygen transport, and survival. *Ann Emerg Med* **49**: 88-98, 98.e81-82, 2007.

30. Tyml K, Budreau CH. A new preparation of rat extensor digitorum longus muscle for intravital investigation of the microcirculation. *International journal of microcirculation, clinical and experimental / sponsored by the European Society for Microcirculation* **10**: 335-343, 1991.

31. Wilson DF, Erecińska M, Drown C, Silver IA. The oxygen dependence of cellular energy metabolism. *Archives of Biochemistry and …*, 1979.

32. Wilson DF, Harrison DK, Vinogradov SA. Oxygen, pH, and mitochondrial oxidative phosphorylation. *Journal of applied physiology (Bethesda, Md : 1985)* **113**: 1838-1845, 2012.

Table 1: Summary of network geometry parameters.

Statistical summary of network geometry data.

	Tissue Volume Dimensions (μm x μm x μm)	Number of Vessel Segments	Mean Capillary Segment Length (μm)	Capillary Length Density (mm x mm^3)
Network I	84 x 168 x 342	25	107.4 ± 82.7	554.2
Network II	70 x 157 x 268	20	100.9 ± 74.7	684.8

This article is protected by copyright. All rights reserved.

Accepted Article

Table 2. Variables for Network II simulations outlining the four different levels of perfusion loss; high consumption simulations are indicated with associated increasing levels of RBC supply rate ranging from baseline RBC supply rate to 4X times baseline RBC flux.

Network I Simulations	% FCD Loss	Consumption - M_0 (mL O_2/mL tissue/s)	RBC Supply Rate (mL RBC/mL tissue/s)	Mean Pressure Drop (mmHg)
Baseline	0	1.5E-4	8.25E-04	3.00
6.7% FCD Loss	6.7	1.5E-4	7.67E-04	3.00
Control, SR Matched to 6.7% FCD Loss	0	1.5E-4	7.67E-04	2.80
20% FCD Loss	20	1.5E-4	7.43E-04	3.00
Control, SR Matched to 20% FCD Loss	0	1.5E-4	7.43E-04	2.71
26.7 FCD Loss	26.7	1.5E-4	6.83E-04	3.00
Control, SR Matched to 26.7% FCD Loss	0	1.5E-4	6.83E-04	2.50
40% FCD Loss	40	1.5E-4	6.07E-04	3.00
Control, SR Matched to 40% FCD Loss	0	1.5E-4	6.07E-04	2.23
40% FCD Loss, Baseline SR	40	1.5E-4	8.25E-04	4.03
40% FCD Loss, High Consumption, Baseline SR	40	3.0E-4	8.25E-04	4.03
Control, 0% FCD Loss, High Consumption, Baseline SR	0	3.0E-4	8.25E-04	3.00
40% FCD Loss, High Consumption, 2X SR	40	3.0E-4	1.65E-03	7.93
Control, 0% FCD Loss, High Consumption, 2X SR	0	3.0E-4	1.65E-03	5.92
40% FCD Loss, High Consumption, 3.5X SR	40	3.0E-4	2.89E-03	13.74
Control, 0% FCD Loss, High Consumption, 3.5 SR	0	3.0E-4	2.89E-03	10.29
40% FCD Loss, High Consumption, 4X	40	3.0E-4	3.30E-03	15.69

This article is protected by copyright. All rights reserved.

SR				
Control, 0% FCD Loss, High Consumption, 4X SR	0	3.0E-4	3.30E-03	11.75

Table 3. Variables for Network II simulations outlining the four different levels of perfusion loss; high consumption simulations are indicated with associated increasing levels of RBC supply rate ranging from baseline RBC supply rate to 4X times baseline RBC flux.

Network II Simulations	% FCD Loss	Consumption - M_0 (mL O_2/mL tissue/s)	RBC Supply Rate (mL RBC/mL tissue/s)	Mean Pressure Drop (mmHg)
Baseline	0	1.5E-4	6.84E-04	1.98
7.1% FCD Loss	7.1	1.5E-4	6.62E-04	1.98
Control, SR Matched to 7.1% FCD Loss	0	1.5E-4	6.62E-04	1.92
21.4% FCD Loss	21.4	1.5E-4	6.12E-04	1.98
Control, SR Matched to 21.4% FCD Loss	0	1.5E-4	6.12E-04	1.78
28.6 FCD Loss	28.6	1.5E-4	5.91E-04	1.98
Control, SR Matched to 28.6% FCD Loss	0	1.5E-4	5.91E-04	1.72
42.9% FCD Loss	42.9	1.5E-4	4.37E-04	1.98
Control, SR Matched to 42.9% FCD Loss	0	1.5E-4	4.37E-04	1.30
42.9% FCD Loss, Baseline SR	42.9	1.5E-4	6.84E-04	2.96
42.9% FCD Loss, High Consumption, Baseline SR	42.9	3.0E-4	6.84E-04	2.96
Control, 0% FCD Loss, High Consumption, Baseline SR	0	3.0E-4	6.84E-04	1.98

Accepted Article

This article is protected by copyright. All rights reserved.

Accepted Article

42.9% FCD Loss, High Consumption, 2X SR	42.9	3.0E-4	1.37E-03	5.70
Control, 0% FCD Loss, High Consumption, 2X SR	0	3.0E-4	1.37E-03	3.88
42.9% FCD Loss, High Consumption, 3.5X SR	42.9	3.0E-4	2.39E-03	8.41
Control, 0% FCD Loss, High Consumption, 3.5 SR	0	3.0E-4	2.39E-03	6.72
42.9% FCD Loss, High Consumption, 4X SR	42.9	3.0E-4	2.74E-03	11.13
Control, 0% FCD Loss, High Consumption, 4X SR	0	3.0E-4	2.74E-03	7.67

Table 4. List of constants and values used in oxygen transport simulations.

Constant	Value
α	3.89 E-5 ml O_2 ml^{-1} $mmHg^{-1}$
α_b	2.82 E-5 ml O_2 ml^{-1} $mmHg^{-1}$
C	0.52 ml O_2 ml^{-1}
D	2.41 E-5 cm^2 s^{-1}
P_{cr}	0.5 mmHg
c_{Mb}	1.02 E-2 ml O_2 ml^{-1}
D_{Mb}	3 E-7 cm^2 s^{-1}
P_{50}	37 mmHg
$P_{50,Mb}$	5.3 mmHg

This article is protected by copyright. All rights reserved.

Accepted Article

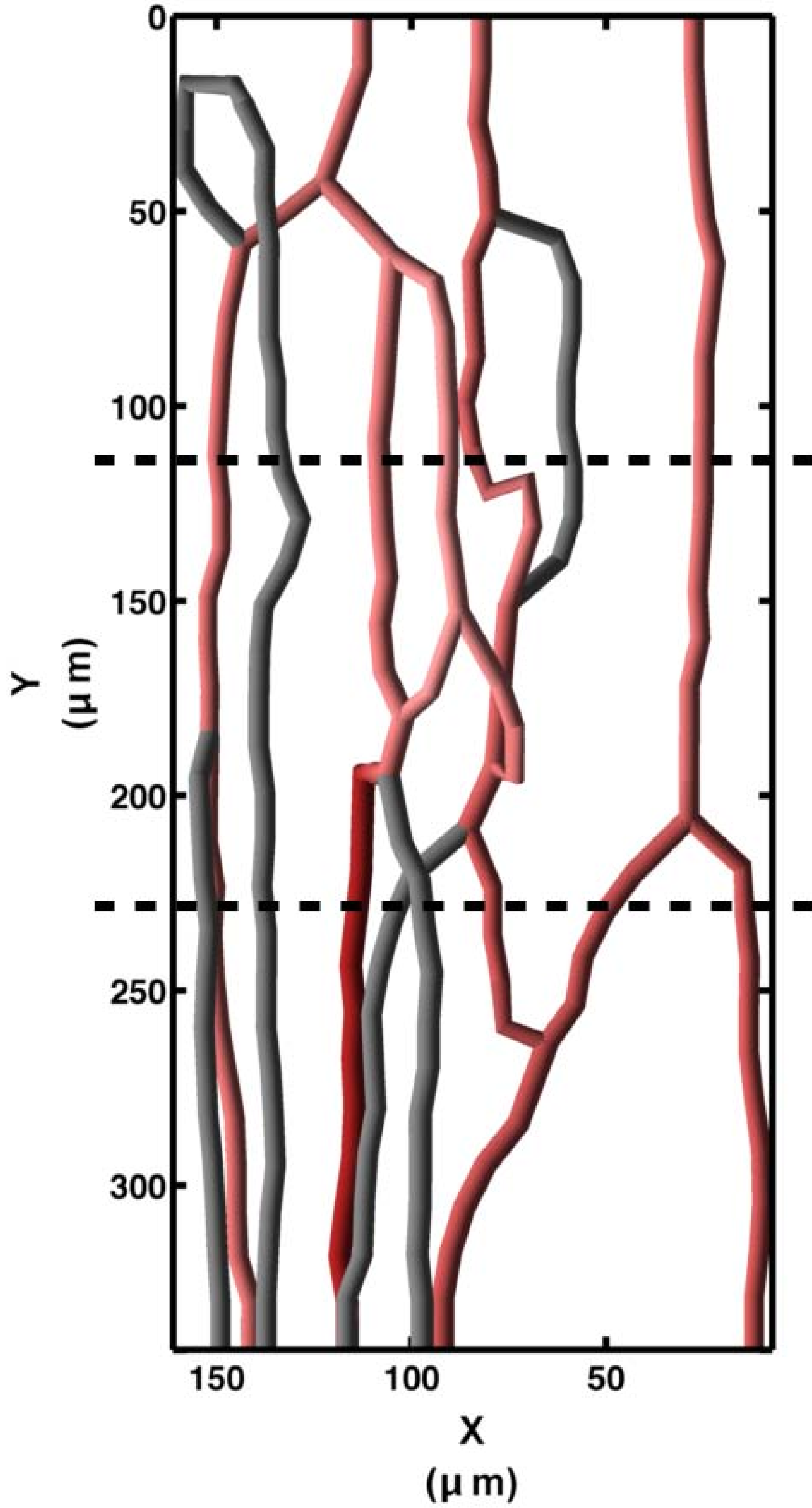

This article is protected by copyright. All rights reserved.

Accepted Article

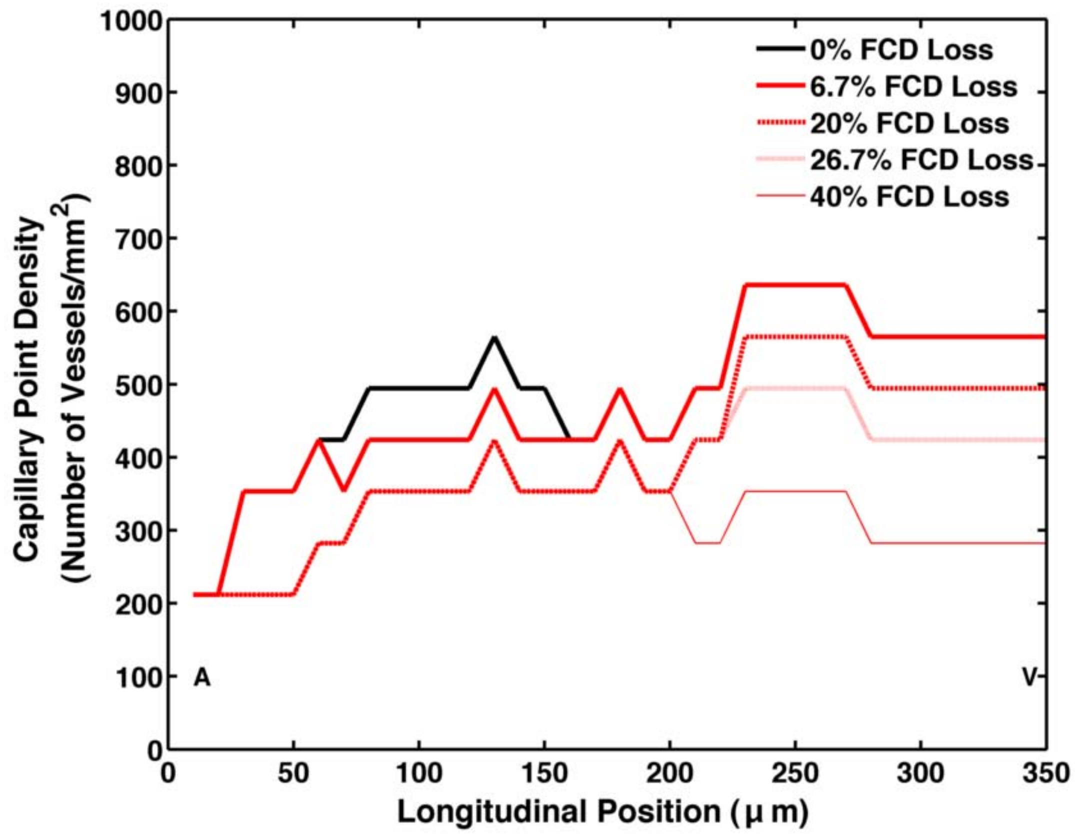

This article is protected by copyright. All rights reserved.

Accepted Article

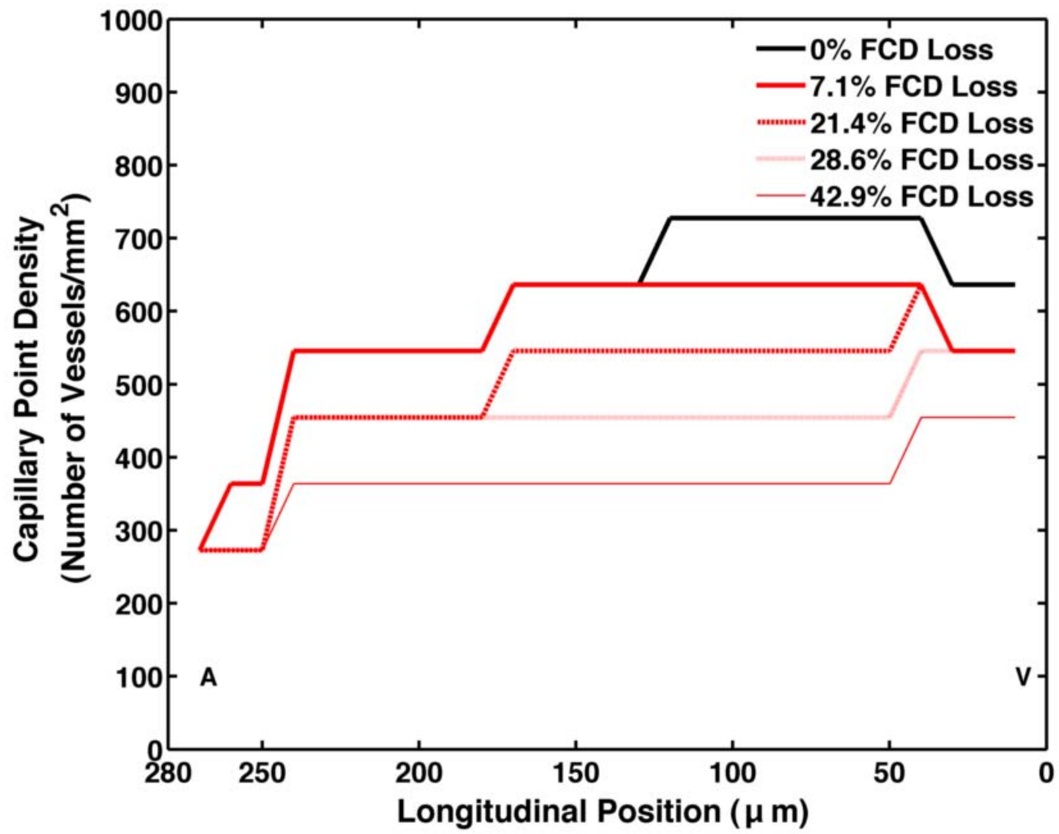

This article is protected by copyright. All rights reserved.

Accepted Article

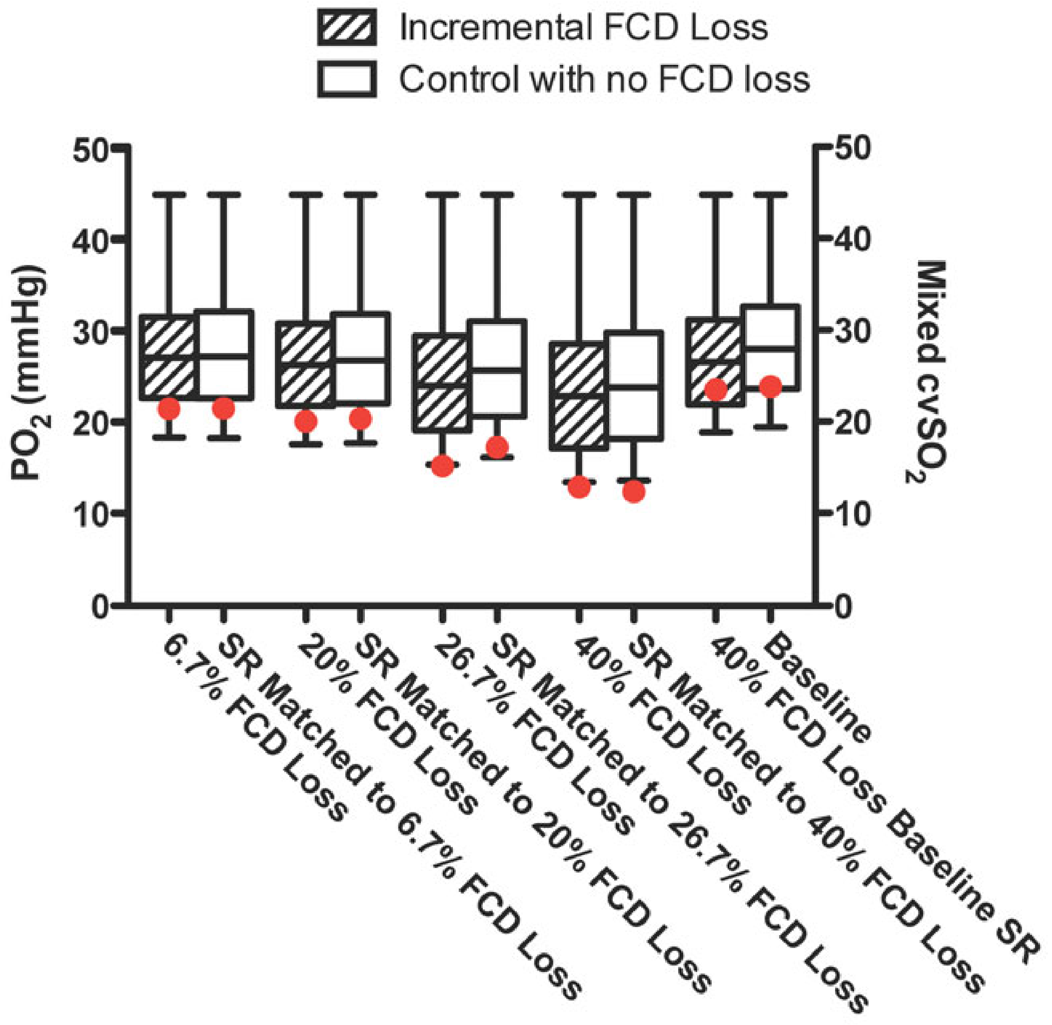

This article is protected by copyright. All rights reserved.

Accepted Article

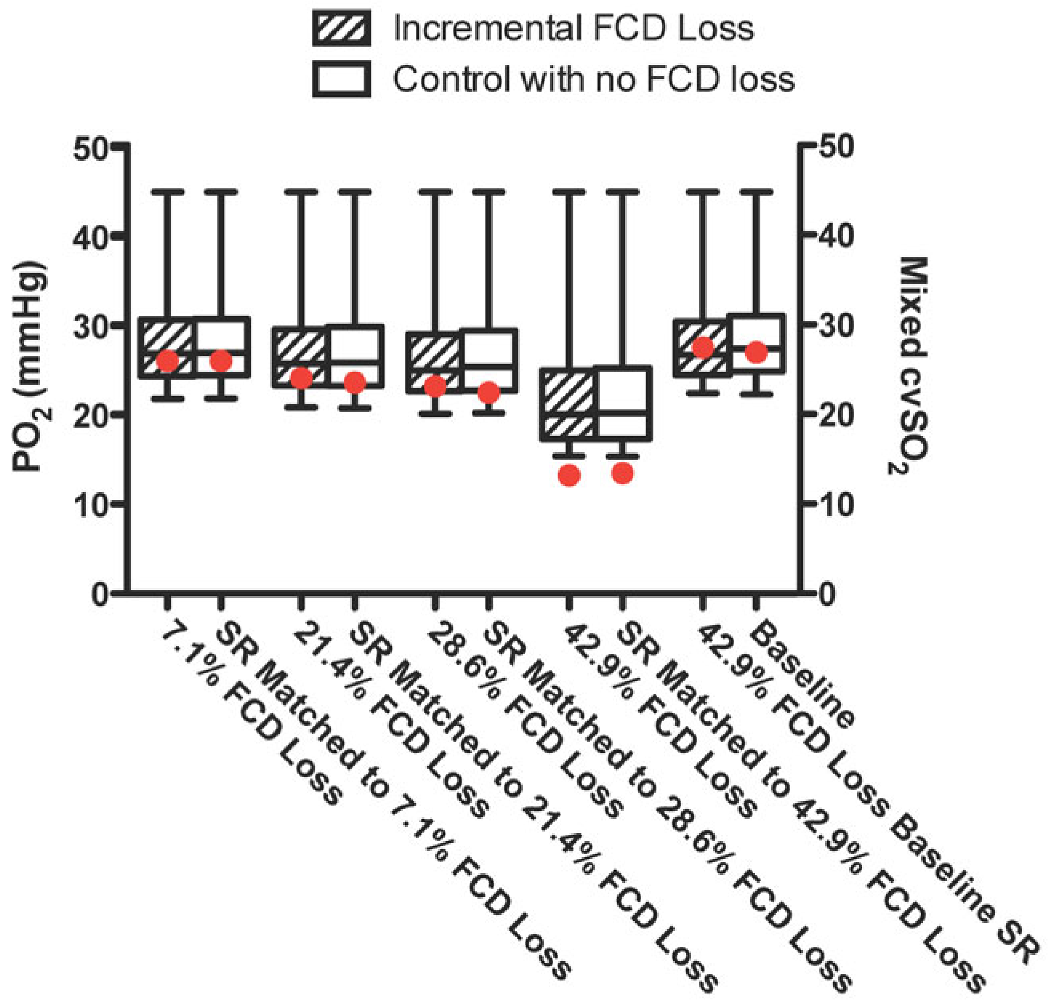

This article is protected by copyright. All rights reserved.

Accepted Article

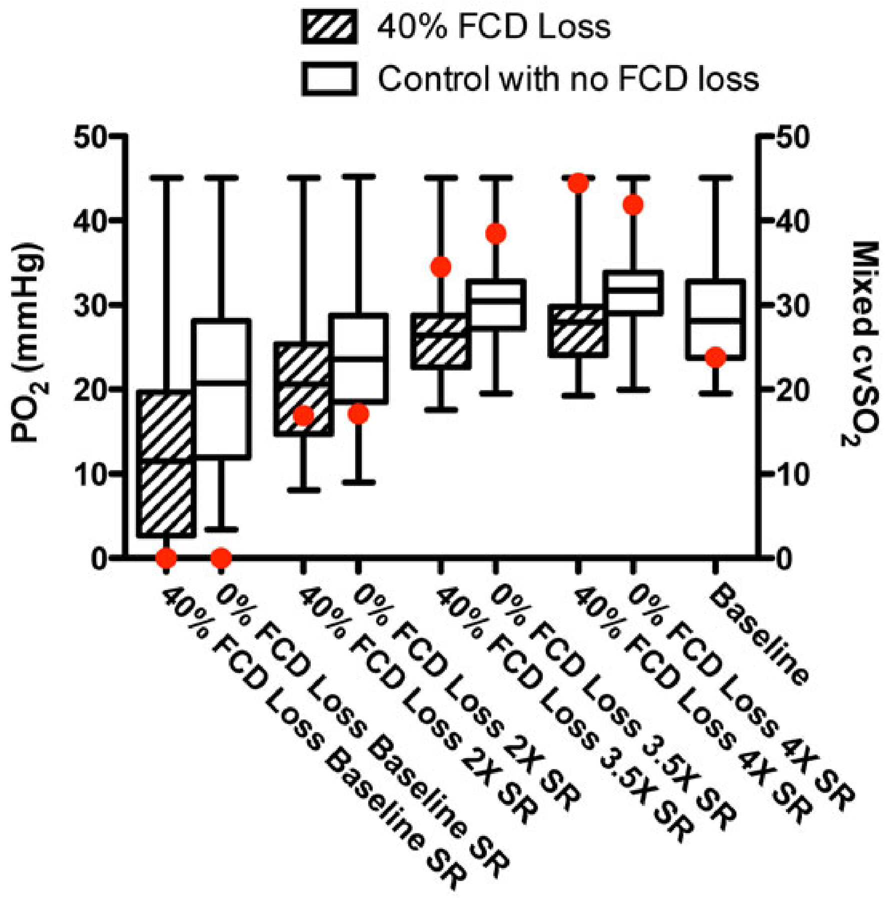

This article is protected by copyright. All rights reserved.

Accepted Article

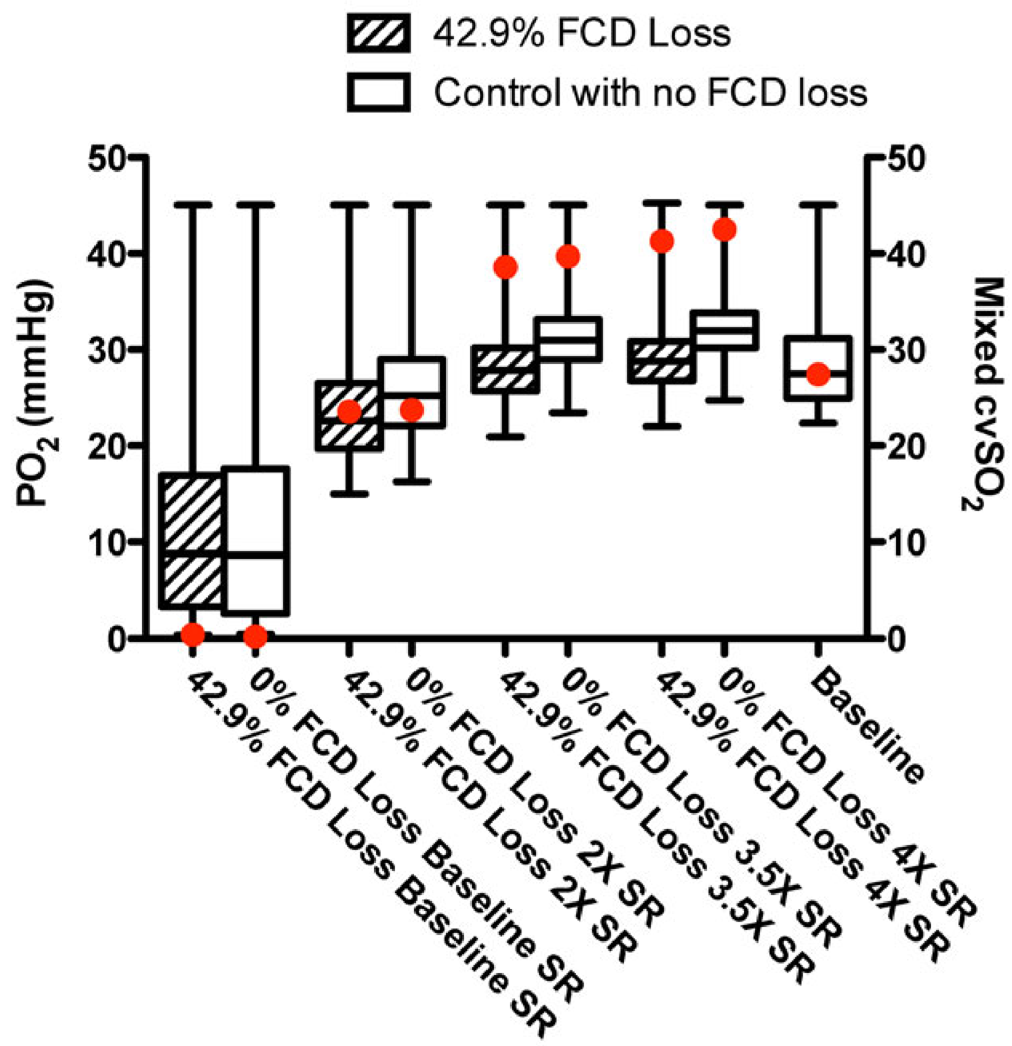

This article is protected by copyright. All rights reserved.

Accepted Article

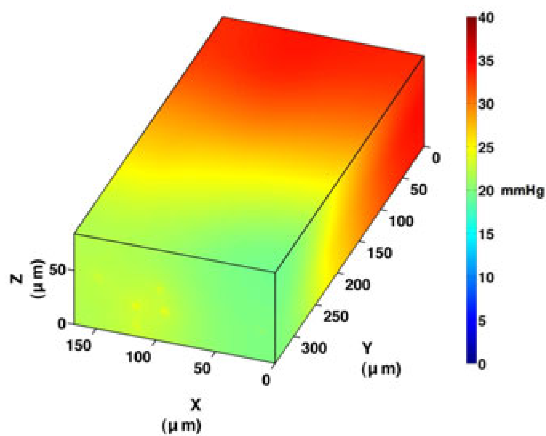

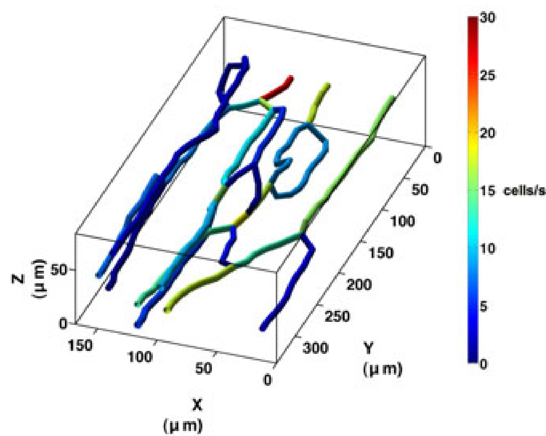

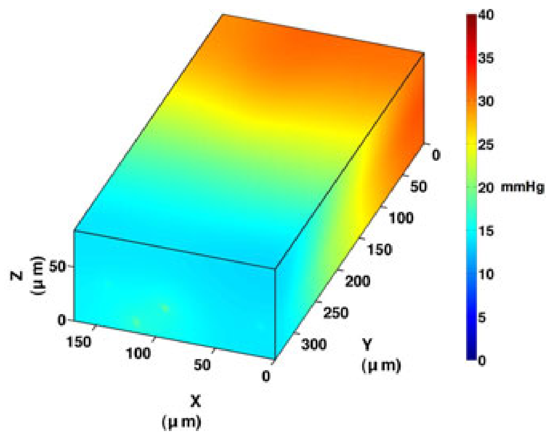

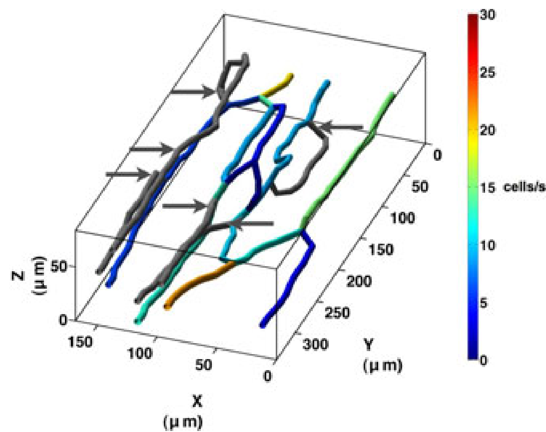

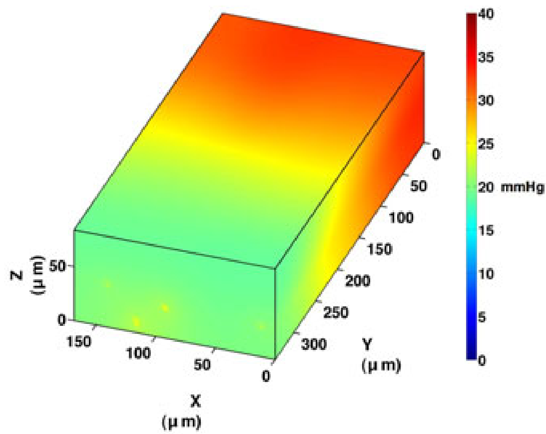

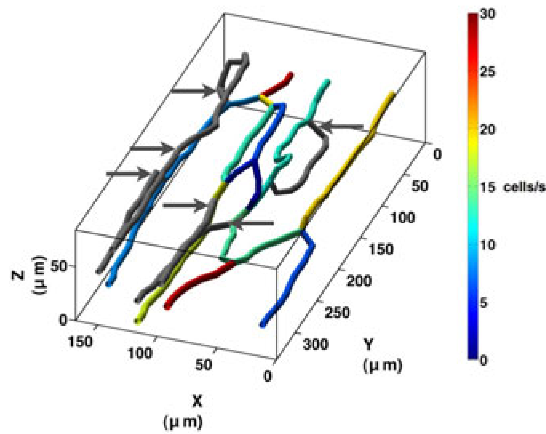

This article is protected by copyright. All rights reserved.

Accepted Article

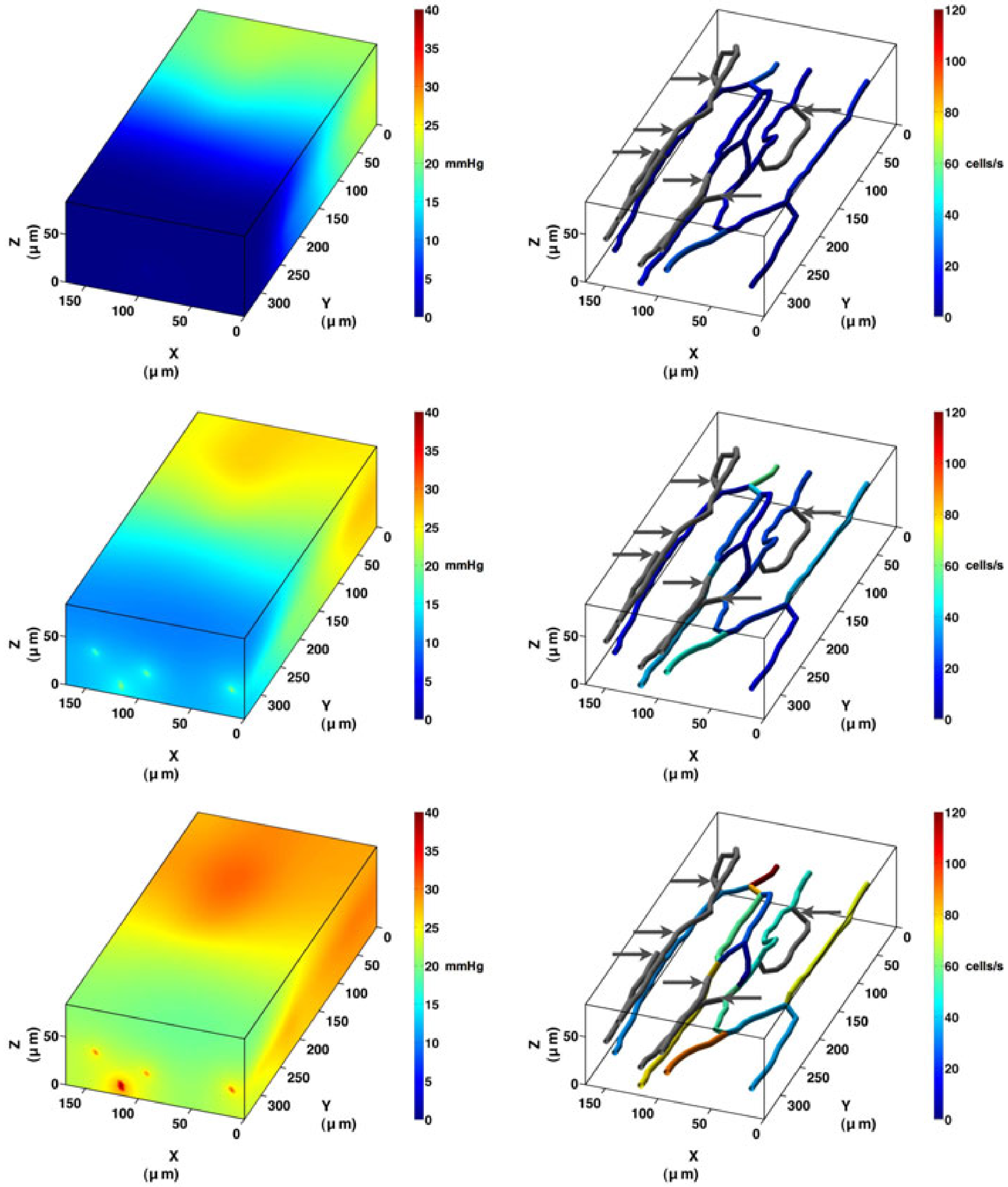

This article is protected by copyright. All rights reserved.